Partially-time-ordered Schwinger-Keldysh loop expansion of coherent nonlinear optical susceptibilities

Shaul Mukamel
Department of Chemistry, University of California, Irvine, California 92697, USA
(Received 29 May 2007; published 5 February 2008)

A compact correlation-function expansion is developed for n-order optical susceptibilities in the frequency domain using the Keldysh-Schwinger loop. By not keeping track of the relative time ordering of bra and ket interactions at the two branches of the loop, the resulting expressions contain only $n+1$ basic terms, compared to the 2^n terms required for a fully-time-ordered density matrix description. Superoperator Green's function expressions for $\chi^{(n)}$ derived using both expansions reflect different types of interferences between pathways. These are demonstrated for correlation-induced resonances in four-wave-mixing signals.

DOI: 10.1103/PhysRevA.77.023801 PACS number(s): 42.65.An, 82.53.Kp

I. INTRODUCTION

Time-ordered expansions form the basis for the perturbative calculation of static and dynamical properties of interacting many-body systems. The nonlinear response to a sequence of n short (impulsive) pulses is most naturally calculated in real (physical) time. The resulting response functions contain 2^n basic terms, stemming from the fact that each interaction can occur either with the ket or with the bra of the system density matrix. This fully time-ordered expansion is routinely used for computing ultrafast (femtosecond) optical signals in molecules, semiconductors, and other materials. The physical picture is recast in terms of the density matrix in Liouville space. Many-body theory of externally driven systems is in contrast commonly formulated using nonequilibrium Green's functions which act in Hilbert space [1–5]. Time ordering is then maintained on an artificial Keldysh-Schwinger loop [6,7], which corresponds to both forward and backward evolution in physical time and forms the basis for perturbative diagrammatic techniques. The loop provides a formal bookkeeping device for various interactions. We only keep track of the number of interactions with the ket and the bra but not of their relative time ordering. The nonlinear response function recast using these artificial (loop) time variables has then a considerably reduced number of terms, $n+1$. Time-domain optical experiments performed using impulsive ultrashort pulses may be described on the loop, but the required transformation from loop-to-real-time variables makes it hard to attribute physical meaning to the various terms [8].

In this paper we show that the loop time ordering is most suitable for computing nonlinear susceptibilities in the frequency domain, where real-time ordering is not maintained in any case. The frequency variables are directly conjugated to the various delay periods along the loop. In Sec. II we derive the correlation-function loop expressions for the third-order susceptibility. Since the loop expansion is much more compact, it may be advantageous to perform many-body calculations in the frequency domain on the loop and then switch to the time domain by a Fourier transform. This way one may exploit the full power of many-body Green's function techniques. These expressions are then recast in Sec. III using a diagrammatic representation in terms of superoperators in Liouville space. The loop and the time-ordered expressions are compared in Sec. IV and shown to contain a different structure of resonances. A superficial look at the two types of expressions may suggest that they predict different types of resonances. This is however misleading since the various terms interfere. Consequently, some apparent resonances may cancel and others may be induced by dephasing processes. Simple diagrammatic rules are provided which allow one to compute the partially-time-ordered expressions. These subtle effects are illustrated in Sec. V by applying this formalism to study correlation-induced resonances in four-wave mixing. The four point dipole correlation function is calculated for a multilevel system whose energy levels fluctuate by coupling to a Brownian oscillator bath. The model allows for an arbitrary degree of correlation between these fluctuations. The expressions may not be generally factorized into products of either real-time delays or loop delays and the resulting complex pattern of resonances may not be attributed to specific time delays. When these fluctuations are negligible the loop expressions best reveal the resonances. In the limit of fast fluctuations (homogeneous dephasing) the real-time expressions show these resonances. These subtle effects are demonstrated in Sec. V where we illustrate the different role of interference in the two types of expansion. We conclude by a discussion of these results in Sec. VI.

II. NONLINEAR SUSCEPTIBILITIES ON THE KELDYSH LOOP

We consider a system interacting with an external electric optical field $E(t)$. The coupling Hamiltonian is $H_{int}=-E(t)V$, where V is the dipole operator. The nonlinear polarization $P^{(n)}$ has $n+1$ terms [9,10]

$$P^{(n)}(t)=\sum_{m=0}^{n}\langle\psi^{(n-m)}(t)|V|\psi^{(m)}(t)\rangle. \tag{1}$$

Here $|\psi^{(m)}\rangle$ is the perturbed wave function to m order in the external field. We shall carry out the calculation for the third-order response, $n=3$. The generalization to n order is straightforward. The field consists of three modes and expanded as

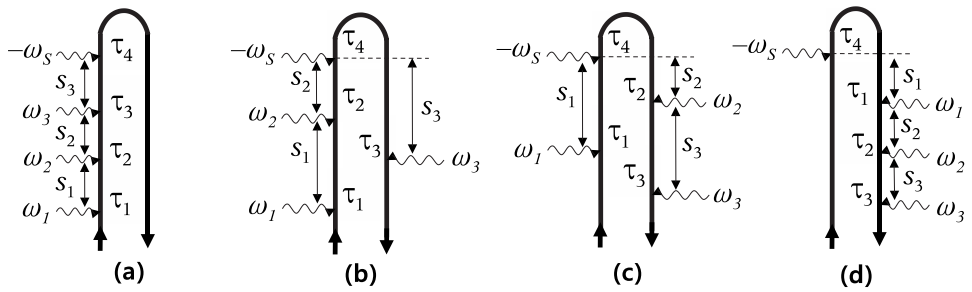

FIG. 1. The four-loop diagrams for $\chi^{(3)}$ representing P_a, P_b, P_c, and P_d in Eq. (3). The loop expansion does not keep track of the relative time ordering of the bra and the ket. s_1, s_2, and s_3 are the time intervals ordered along the loop.

$$E(t) = \sum_{j=1}^{3} E_j(t)\exp(-i\omega_j t) + \text{c.c.} \tag{2}$$

Equation (1) now has four terms which correspond to $m=3,2,1,0$ and are represented by the Feynman diagrams shown in Figs. 1(a)–1(d), respectively. The system interacts with the fields E_1, E_2, and E_3 at times τ_1, τ_2, and τ_3, respectively, and the polarization is calculated at τ_4 by integrating over the time variables τ_j. Each diagram represents a different ordering of τ_j along the loop.

Fourier transform of Eq. (1) to the frequency domain gives

$$P^{(3)}(\omega_s) \equiv \int_{-\infty}^{\infty} dt\, \exp(i\omega_s t) P^{(3)}(t) = P_a + P_b + P_c + P_d, \tag{3}$$

where

$$P_a(\omega_s) = \int_{-\infty}^{\infty} d\tau_4 \int_{-\infty}^{\tau_4} d\tau_3 \int_{-\infty}^{\tau_3} d\tau_2 \int_{-\infty}^{\tau_2} d\tau_1 E_1(\tau_1)E_2(\tau_2)E_3(\tau_3) \times F(\tau_4,\tau_3,\tau_2,\tau_1)\exp(-i\omega_1\tau_1 - i\omega_2\tau_2 - i\omega_3\tau_3 + i\omega_s\tau_4), \tag{4}$$

$$P_b(\omega_s) = -\int_{-\infty}^{\infty} d\tau_4 \int_{-\infty}^{\tau_4} d\tau_2 \int_{-\infty}^{\tau_2} d\tau_1 \int_{-\infty}^{\tau_4} d\tau_3 E_1(\tau_1)E_2(\tau_2)E_3(\tau_3) \times F(\tau_3,\tau_4,\tau_2,\tau_1)\exp(-i\omega_1\tau_1 - i\omega_2\tau_2 - i\omega_3\tau_3 + i\omega_s\tau_4), \tag{5}$$

$$P_c(\omega_s) = \int_{-\infty}^{\infty} d\tau_4 \int_{-\infty}^{\tau_4} d\tau_1 \int_{-\infty}^{\tau_4} d\tau_2 \int_{-\infty}^{\tau_2} d\tau_3 E_1(\tau_1)E_2(\tau_2)E_3(\tau_3) \times F(\tau_3,\tau_2,\tau_4,\tau_1)\exp(-i\omega_1\tau_1 - i\omega_2\tau_2 - i\omega_3\tau_3 + i\omega_s\tau_4), \tag{6}$$

$$P_d(\omega_s) = -\int_{-\infty}^{\infty} d\tau_4 \int_{-\infty}^{\tau_4} d\tau_1 \int_{-\infty}^{\tau_1} d\tau_2 \int_{-\infty}^{\tau_2} d\tau_3 E_1(\tau_1)E_2(\tau_2)E_3(\tau_3) \times F(\tau_3,\tau_2,\tau_1,\tau_4)\exp(-i\omega_1\tau_1 - i\omega_2\tau_2 - i\omega_3\tau_3 + i\omega_s\tau_4). \tag{7}$$

Here we have defined the correlation function

$$F(\tau_4,\tau_3,\tau_2,\tau_1) \equiv \left(\frac{i}{\hbar}\right)^3 \text{Tr}[V(\tau_4)V(\tau_3)V(\tau_2)V(\tau_1)\rho] \equiv \left(\frac{i}{\hbar}\right)^3 \langle V(\tau_4)V(\tau_3)V(\tau_2)V(\tau_1)\rangle, \tag{8}$$

where ρ is the equilibrium density matrix and $V(t)$ are interaction picture operators with respect to the free system Hamiltonian H,

$$V(t) = \exp(iHt)V\exp(-iHt). \tag{9}$$

By introducing the Heavyside step functions $\theta(t)$ we can set all time integration limits from $-\infty$ to ∞, and combine the four terms as

$$P^{(3)}(\omega_s) = \int_{-\infty}^{\infty}\int_{-\infty}^{\infty}\int_{-\infty}^{\infty}\int_{-\infty}^{\infty} d\tau_4 d\tau_3 d\tau_2 d\tau_1 \exp(-i\omega_1\tau_1 - i\omega_2\tau_2 - i\omega_3\tau_3 + i\omega_s\tau_4) \times [\theta(\tau_{21})\theta(\tau_{32})\theta(\tau_{43})F(\tau_4,\tau_3,\tau_2,\tau_1)E_1(\tau_1)E_2(\tau_2)E_3(\tau_3) - \theta(\tau_{21})\theta(\tau_{42})\theta(\tau_{43})F(\tau_3,\tau_4,\tau_2,\tau_1)E_1(\tau_1)E_2(\tau_2)E_3(\tau_3) + \theta(\tau_{41})\theta(\tau_{42})\theta(\tau_{23})F(\tau_3,\tau_2,\tau_4,\tau_1)E_1(\tau_1)E_2(\tau_2)E_3(\tau_3) - \theta(\tau_{41})\theta(\tau_{12})\theta(\tau_{23})F(\tau_3,\tau_2,\tau_1,\tau_4)E_1(\tau_1)E_2(\tau_2)E_3(\tau_3)]. \tag{10}$$

The third order susceptibility $\chi^{(3)}$ is defined by [9]

$$P^{(3)}(\omega_s) = \int\int\int d\omega_1 d\omega_2 d\omega_3 \chi^{(3)}(-\omega_s;\omega_1,\omega_2,\omega_3)E_1(\omega_1)E_2(\omega_2)E_3(\omega_3)\delta(\omega_s - \omega_1 - \omega_2 - \omega_3), \tag{11}$$

where

$$E_j(\omega) = \int dt E_j(t)\exp(i\omega t). \tag{12}$$

By comparing Eqs. (10) and (11) we obtain

$$\begin{aligned}\chi^{(3)}(-\omega_s;\omega_1,\omega_2,\omega_3) = \frac{1}{(2\pi)^2}\sum_p \int_0^\infty ds_1 \int_0^\infty ds_2 \int_0^\infty ds_3 \{&F(s_1+s_2+s_3,s_1+s_2,s_1,0)\exp[i\omega_1 s_1 + i(\omega_1+\omega_2)s_2 + i(\omega_1+\omega_2+\omega_3)s_3] \\ &- F(s_1+s_2-s_3,s_1+s_2,s_1,0)\exp[i\omega_1 s_1 + i(\omega_1+\omega_2)s_2 - i(\omega_1-\omega_s+\omega_2)s_3] \\ &+ F(s_1-s_2-s_3,s_1-s_2,s_1,0)\exp[i\omega_1 s_1 - i(\omega_1-\omega_s)s_2 - i(\omega_1-\omega_s+\omega_2)s_3] - F(0,s_3,s_3+s_2,s_3+s_2+s_1) \\ &\times\exp[i\omega_s s_1 - i(-\omega_s+\omega_1)s_2 - i(-\omega_s+\omega_1+\omega_2)s_3]\}.\end{aligned} \tag{13}$$

In Eq. (13) s_j are the time intervals between the various interactions along the loop. The frequency arguments of $\chi^{(3)}$ are thus naturally connected with these variables. Time ordering is maintained on the loop but not in real (physical) time. Σ_p denotes the sum over all 3! permutations of $\omega_1,\omega_2,\omega_3$.

We shall now compare this result with the fully time-ordered expressions for the response functions obtained by expanding the density matrix [8]. Generally $S^{(n)}$ has 2^n terms. For $n=3$ we obtain

$$\begin{aligned}P^{(3)}(t) = \int_0^\infty dt_1 \int_0^\infty dt_2 \int_0^\infty dt_3 S^{(3)}(t_3,t_2,t_1) \\ \times E_1(t-t_3-t_2-t_1)E_2(t-t_3-t_2)E_3(t-t_3).\end{aligned} \tag{14}$$

Unlike Eq. (10), E_1, E_2, and E_3 now represent the first, second, and third pulse (chronologically ordered)

$$\begin{aligned}S^{(3)}(t_3,t_2,t_1) = \left(\frac{i}{\hbar}\right)^3 \theta(t_1)\theta(t_2)\theta(t_3) \\ \times\langle[[[V(t_1+t_2+t_3),V(t_2+t_3)],V(t_3)],V(0)]\rangle.\end{aligned} \tag{15}$$

Using Eq. (8), Eq. (15) gives

$$\begin{aligned}S^{(3)}(t_3,t_2,t_1) = \theta(t_1)\theta(t_2)\theta(t_3)[&F(t_1,t_1+t_2,t_1+t_2+t_3,0) \\ &+ F(0,t_1+t_2,t_1+t_2+t_3,t_1) \\ &+ F(0,t_1,t_1+t_2+t_3,t_1+t_2) \\ &+ F(t_1+t_2+t_3,t_1+t_2,t_1,0)] + \text{c.c.}\end{aligned} \tag{16}$$

The third-order susceptibility is finally given by

$$\begin{aligned}\chi^{(3)}(-\omega_s;\omega_1,\omega_2,\omega_3) = \frac{1}{(2\pi)^2}\sum_p \int_0^\infty dt_1 \int_0^\infty dt_2 \int_0^\infty dt_3 \\ \times S^{(3)}(t_3,t_2,t_1)\exp[i\omega_1 t_1 + i(\omega_1+\omega_2)t_2 \\ + i(\omega_1+\omega_2+\omega_3)t_3].\end{aligned} \tag{17}$$

The loop expression, Eq. (13), generally has $n+1$ terms (4 for $n=3$), whereas the time-ordered expression, Eq. (17), has a much larger number 2^n (8 for $n=3$). Note that the signal frequency ω_s does enter explicitly in the integrations in Eq. (13) but not in Eq. (17). t_j are intervals between successive interactions in real time and are most convenient for impulsive techniques. s_j represent intervals along the loop and are particularly useful for frequency domain susceptibilities. This will be demonstrated next.

III. SUPEROPERATOR EXPRESSIONS FOR SUSCEPTIBILITIES

By expressing Eq. (8) in terms of superoperators we can derive a more compact Green's function expressions for the susceptibilities using a simple diagrammatic representation. Below we briefly survey the basic elements of the Liouville space superoperator formalism [8,11–13]. With each ordinary (Hilbert space) operator, Q, we associate two superoperators, denoted as Q_L (left) and Q_R (right) defined through their left or right action on some Hilbert space operator X,

$$Q_L X \equiv QX, \quad Q_R X \equiv XQ. \tag{18}$$

We further define the linear combinations of these superoperators $Q^+ \equiv (Q_L+Q_R)/2$ and $Q^- \equiv Q_L - Q_R$. Thus a $+(-)$ operation in Liouville space corresponds to an anticommutation (commutation) operation in Hilbert space, $Q^+X \equiv (QX+XQ)/2$ and $Q^-X \equiv QX-XQ$.

The interaction picture for superoperators is defined by

$$U_\alpha(t) = \exp(iLt)U_\alpha\exp(-iLt), \quad \alpha = L,R, \tag{19}$$

where $LA \equiv [H,A]$ is the Liouville operator.

When substituting Eq. (9) in Eq. (8) we obtain

$$\begin{aligned}F(\tau_4,\tau_3,\tau_2,\tau_1) = \left(\frac{i}{\hbar}\right)^3 \text{Tr}[&\exp(-iH\tau_{14}) \\ &\times V\exp(-iH\tau_{43})V\exp(-iH\tau_{32})V \\ &\times\exp(-iH\tau_{21})V\rho].\end{aligned} \tag{20}$$

Note that all interactions in Eq. (8) are from the left, i.e., they act on the ket of the density matrix. We can thus recast it using "left" superoperators as follows:

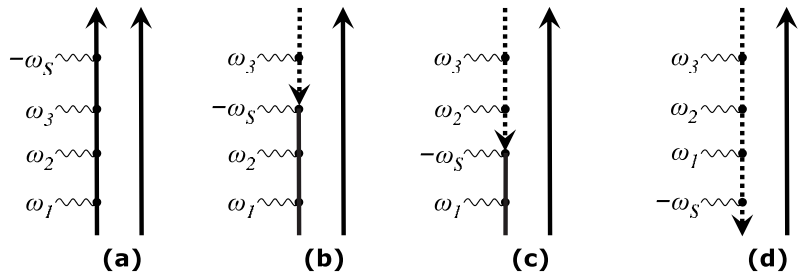

FIG. 2. Unfolded loop diagrams corresponding to diagrams 1(a), 1(b), 1(c), and 1(d). Equations (25) and (32) can be derived directly from these diagrams using the rules given in the text. All interactions are now from the left (ket), while the bra propagates freely. Solid and dashed lines represent forward and backward propagation, respectively.

$$F(\tau_4,\tau_3,\tau_2,\tau_1)=\left(\frac{i}{\hbar}\right)^3 \mathrm{Tr}[V_L(\tau_4)V_L(\tau_3)V_L(\tau_2)V_L(\tau_1)\rho]. \tag{21}$$

Combining Eqs. (19) and (20) gives

$$\begin{aligned}F(\tau_4,\tau_3,\tau_2,\tau_1)=\left(\frac{i}{\hbar}\right)^3 \mathrm{Tr}[&\exp(iL\tau_4)\\ &\times V_L\exp(-iL\tau_{43})V_L\exp(-iL\tau_{32})\\ &\times V_L\exp(-iL\tau_{21})V_L\exp(-iL\tau_1)\rho].\end{aligned}$$

When $\exp(-iL\tau_1)$ acts on the equilibrium density matrix ρ it does not affect it and gives ρ. Similarly, $\exp(iL\tau_4)$ when acting to the left will give 1 under the trace. These two propagators can thus be dropped and we finally obtain

$$\begin{aligned}&F(\tau_4,\tau_3,\tau_2,\tau_1)\\ &\quad=\left(\frac{i}{\hbar}\right)^3 \mathrm{Tr}[V_L\exp(-iL\tau_{43})V_L\\ &\qquad\times\exp(-iL\tau_{32})V_L\exp(-iL\tau_{21})V_L\rho].\end{aligned} \tag{22}$$

Using Eq. (22), the correlation functions in Eq. (13) now become

$$\begin{aligned}F(s_1+s_2+s_3,s_1+s_2,s_1,0)&=\langle V_L\mathcal{G}(s_3)V_L\mathcal{G}(s_2)V_L\mathcal{G}(s_1)V_L\rangle,\\ F(s_1+s_2-s_3,s_1+s_2,s_1,0)&=\langle V_L\mathcal{G}^\dagger(s_3)V_L\mathcal{G}(s_2)V_L\mathcal{G}(s_1)V_L\rangle,\\ F(s_1-s_2-s_3,s_1-s_2,s_1,0)&=\langle V_L\mathcal{G}^\dagger(s_3)V_L\mathcal{G}^\dagger(s_2)V_L\mathcal{G}(s_1)V_L\rangle,\\ F(0,s_3,s_3+s_2,s_3+s_2+s_1)&=\langle V_L\mathcal{G}^\dagger(s_3)V_L\mathcal{G}^\dagger(s_2)V_L\mathcal{G}^\dagger(s_1)V_L\rangle.\end{aligned} \tag{23}$$

Here we have made use of the fact that all s variables are positive and represent "forward" propagation along the loop,

$$\begin{aligned}\mathcal{G}(s)&=\left(-\frac{i}{\hbar}\right)\theta(s)\exp(-iLs-\eta s),\\ \mathcal{G}^\dagger(s)&=\left(\frac{i}{\hbar}\right)\theta(s)\exp(iLs-\eta s).\end{aligned} \tag{24}$$

We reiterate that ordering on the loop does not represent ordering in real time. Using superoperators we were able to recast F in terms of three propagators [in Hilbert space F, Eq. (20) has four propagators]. By substituting Eq. (23) in Eq. (13) we obtain

$$\begin{aligned}\chi^{(3)}(-\omega_s;\omega_1,\omega_2,\omega_3)=-\frac{1}{(2\pi)^2}\sum_p[&\langle V_L\mathcal{G}(\omega_1+\omega_2+\omega_3)V_L\mathcal{G}(\omega_1+\omega_2)V_L\mathcal{G}(\omega_1)V_L\rangle\\ &-\langle V_L\mathcal{G}^\dagger(-\omega_s+\omega_1+\omega_2)V_L\mathcal{G}(\omega_1+\omega_2)V_L\mathcal{G}(\omega_1)V_L\rangle\\ &+\langle V_L\mathcal{G}^\dagger(-\omega_s+\omega_1+\omega_2)V_L\mathcal{G}^\dagger(-\omega_s+\omega_1)V_L\mathcal{G}(\omega_1)V_L\rangle\\ &-\langle V_L\mathcal{G}^\dagger(-\omega_s+\omega_1+\omega_2)V_L\mathcal{G}^\dagger(-\omega_s+\omega_1)V_L\mathcal{G}^\dagger(-\omega_s)V_L\rangle].\end{aligned} \tag{25}$$

Here

$$\mathcal{G}(\omega)=\frac{1}{\omega-L+i\eta} \tag{26}$$

is the retarded Green's function and

$$\mathcal{G}^{\dagger}(\omega) = \frac{1}{\omega - L - i\eta} \tag{27}$$

is the advanced Green's function, where η is a positive infinitesimal.

Equation (25) may be represented by the unfolded loop diagrams shown in Fig. 2. These diagrams may be constructed using the following rules:

(i) Each V_L is represented by an arrow acting on the ket from the left.

(ii) Each V_L is associated with one of the frequencies $\pm\omega_1, \pm\omega_2, \pm\omega_3, \pm\omega_s$. Positive frequency $+\omega$ (negative frequency $-\omega$) is represented by an arrow pointing to the right (left).

(iii) There are $(n+1)$ choices for the position of ω_s along the loop, see Eq. (1). Each gives one diagram.

(iv) Each interval "before" ("after") ω_s gives a Green's function $\mathcal{G}(\omega)$ $[\mathcal{G}^{\dagger}(\omega)]$.

(v) The frequency argument of each Green's function is the sum of all "earlier" frequencies along the loop (frequency is cumulative).

(vi) All ω_j other than ω_s can be interchanged, giving $n!$ permutations of $\omega_1 \ldots \omega_n$. Altogether $\chi^{(3)}$ finally has $(n+1)!$ terms.

Finally, for comparison, using the fully-time-ordered expansion, Eq. (15), we have

$$\begin{aligned}\chi^{(3)}(-\omega_s;\omega_1,\omega_2,\omega_3) = -\frac{1}{(2\pi)^2}\sum_p [&\langle V_L\mathcal{G}(\omega_1+\omega_2+\omega_3)V_R\mathcal{G}(\omega_1+\omega_2)V_R\mathcal{G}(\omega_1)V_L\rangle \\ &+\langle [V_L\mathcal{G}(\omega_1+\omega_2+\omega_3)V_R\mathcal{G}(\omega_1+\omega_2)V_L\mathcal{G}(\omega_1)V_R\rangle + \langle V_L\mathcal{G}(\omega_1+\omega_2+\omega_3)V_L\mathcal{G}(\omega_1+\omega_2)V_R\mathcal{G}(\omega_1)V_R\rangle \\ &+\langle V_L\mathcal{G}(\omega_1+\omega_2+\omega_3)V_L\mathcal{G}(\omega_1+\omega_2)V_L\mathcal{G}(\omega_1)V_L\rangle - \langle V_L\mathcal{G}(\omega_1+\omega_2+\omega_3)V_L\mathcal{G}(\omega_1+\omega_2)V_R\mathcal{G}(\omega_1)V_L\rangle \\ &-\langle V_L\mathcal{G}(\omega_1+\omega_2+\omega_3)V_L\mathcal{G}(\omega_1+\omega_2)V_L\mathcal{G}(\omega_1)V_R\rangle - \langle V_L\mathcal{G}(\omega_1+\omega_2+\omega_3)V_R\mathcal{G}(\omega_1+\omega_2)V_L\mathcal{G}(\omega_1)V_L\rangle \\ &-\langle V_L\mathcal{G}(\omega_1+\omega_2+\omega_3)V_R\mathcal{G}(\omega_1+\omega_2)V_R\mathcal{G}(\omega_1)V_R\rangle].\end{aligned} \tag{28}$$

Equation (28) may be represented by the double-sided Feyman diagrams [8] shown in Fig. 3. Note that this expression only contains retarded Green's functions representing forward time evolution, whereas Eq. (25) contains both retarded and advanced Green's functions. A more detailed comparison will be given in the next section.

IV. RESONANCE STRUCTURE AND INTERFERENCE IN THE FULLY-AND PARTIALLY-TIME-ORDERED EXPANSIONS

Consider a multilevel system $a,b,c,\ldots$ interacting with a bath whose Hamiltonian depends on the state of the system. The total eigenstates in the joint system plus bath space are denoted $|a\alpha\rangle, |b\beta\rangle, |c\gamma\rangle$, etc. Note that the manifolds $\{\alpha\},\{\beta\},\{\gamma\}$ diagonalize different bath Hamiltonians and they are not orthogonal to each other. For this model the total Green's function is given by

$$\mathcal{G}(\omega) = \sum_{a\alpha,b\beta} \frac{|a\alpha,b\beta\rangle\rangle\langle\langle a\alpha,b\beta|}{\omega - \omega_{ab} - \omega_{\alpha\beta} + i\eta}, \tag{29}$$

where $\omega_{ab} \equiv \omega_a - \omega_b$ is the transition frequency between states $|a\rangle$ and $|b\rangle$ and $\omega_{\alpha\beta} \equiv \varepsilon_\alpha - \varepsilon_\beta$. We next define the reduced bath Green's function by a partial trace over the system (denoted by a subscript s)

$$\mathcal{G}_{ab}(\omega) \equiv \langle\langle ab|\mathcal{G}(\omega)|ab\rangle\rangle_s. \tag{30}$$

$\mathcal{G}_{ab}(\omega)$ is thus a superoperator in bath space,

$$\mathcal{G}_{ab}(\omega)\sum_{\alpha,\beta} \frac{|\alpha\beta\rangle\rangle\langle\langle\alpha\beta|}{\omega - \omega_{ab} - \omega_{\alpha\beta} + i\eta}. \tag{31}$$

Expanding Eq. (25) in eigenstates gives

$$\begin{aligned}\chi^{(3)}(-\omega_s;\omega_1,\omega_2,\omega_3) = -\frac{1}{(2\pi)^2}\sum_{a,b,c,d} P(a)V_{ad}V_{dc}V_{cb}V_{ba}[&\langle\mathcal{G}_{da}(\omega_1+\omega_2+\omega_3)\mathcal{G}_{ca}(\omega_1+\omega_2)\mathcal{G}_{ba}(\omega_1)\rangle \\ &-\langle\mathcal{G}^{\dagger}_{da}(-\omega_s+\omega_1+\omega_2)\mathcal{G}_{ca}(\omega_1+\omega_2)\mathcal{G}_{ba}(\omega_1)\rangle + \langle\mathcal{G}^{\dagger}_{da}(-\omega_s+\omega_1+\omega_2)\mathcal{G}^{\dagger}_{ca}(-\omega_s+\omega_1)\mathcal{G}_{ba}(\omega_1)\rangle \\ &-\langle\mathcal{G}^{\dagger}_{da}(-\omega_s+\omega_1+\omega_2)\mathcal{G}^{\dagger}_{ca}(-\omega_s+\omega_1)\mathcal{G}^{\dagger}_{ba}(-\omega_1)\rangle].\end{aligned} \tag{32}$$

Here $P(a)$ is the equilibrium population of state $|a\rangle$. For comparison, by expanding the time-ordered expression, Eq. (28), in eigenstates we obtain

$$\chi^{(3)}(-\omega_s;\omega_1,\omega_2,\omega_3) = -\frac{1}{(2\pi)^2}\sum_p \sum_{a,b,c,d} P(a)V_{ad}V_{dc}V_{cb}V_{ba}[\langle \mathcal{G}_{dc}(\omega_1+\omega_2+\omega_3)\mathcal{G}_{db}(\omega_1+\omega_2)\mathcal{G}_{da}(\omega_1)\rangle + \langle \mathcal{G}_{dc}(\omega_1+\omega_2+\omega_3)\mathcal{G}_{db}(\omega_1+\omega_2)\mathcal{G}_{ab}(\omega_1)\rangle + \langle \mathcal{G}_{dc}(\omega_1+\omega_2+\omega_3)\mathcal{G}_{ac}(\omega_1+\omega_2)\mathcal{G}_{ab}(\omega_1)\rangle + \langle \mathcal{G}_{ba}(\omega_1+\omega_2+\omega_3)\mathcal{G}_{ca}(\omega_1+\omega_2)\mathcal{G}_{da}(\omega_1)\rangle - \langle \mathcal{G}_{cb}(\omega_1+\omega_2+\omega_3)\mathcal{G}_{db}(\omega_1+\omega_2)\mathcal{G}_{da}(\omega_1)\rangle - \langle \mathcal{G}_{dc}(\omega_1+\omega_2+\omega_3)\mathcal{G}_{db}(\omega_1+\omega_2)\mathcal{G}_{da}(\omega_1)\rangle - \langle \mathcal{G}_{cb}(\omega_1+\omega_2+\omega_3)\mathcal{G}_{ca}(\omega_1+\omega_2)\mathcal{G}_{da}(\omega_1)\rangle - \langle \mathcal{G}_{ad}(\omega_1+\omega_2+\omega_3)\mathcal{G}_{ac}(\omega_1+\omega_2)\mathcal{G}_{ab}(\omega_1)\rangle]. \quad (33)$$

It is interesting to note that Eq. (32) only suggests resonances with transitions involving the initial state a, ω_{va}, whereas Eq. (33) shows explicitly resonances between any pair of levels $\omega_{\nu\nu'}$. Both expressions are however formally exact and these apparent differences disappear by interferences between various terms that can cancel some resonances or induce new ones. When the dynamics of fluctuations is such that the loop time variables s_1, s_2, s_3 are independent, the products of Green's functions in Eq. (23) can be factorized and Eq. (32) then provides a natural representation for the observed resonances. Similarly, when the physical time delays between pulses t_1, t_2, and t_3 are independent, products of the corresponding Green's functions can be factorized, and Eq. (33) should show the proper resonances. Most generally, neither factorization holds and averages of products of Green's functions must be carefully carried out. This will be illustrated in the next section using a model of multilevel system coupled to a Brownian oscillator bath.

V. CORRELATION-INDUCED RESONANCES IN FOUR-WAVE MIXING

We consider a multilevel system coupled to a harmonic bath and described by the Hamiltonian

$$\hat{H} = \hat{H}_S + \hat{H}_B + \hat{H}_{SB}, \quad (34)$$

where the three terms represent, respectively, the system, the bath, and their interaction.

$$\hat{H}_S = \sum_\nu \varepsilon_\nu |\nu\rangle\langle\nu|, \quad (35)$$

where ε_ν is the energy of eigenstate ν.

The system is linearly coupled to the bath through

$$\hat{H}_{SB} = \sum_\nu \hat{Q}_\nu |\nu\rangle\langle\nu|, \quad (36)$$

where $\hat{Q}_\nu$ is a collective bath coordinate which modulates the energy of state υ.

The response function for this model of diagonal fluctuations can be calculated exactly using the second-order cumulant expansion. Expanding the four point correlation function in the system eigenstates we obtain [14]

$$F(\tau_4,\tau_3,\tau_2,\tau_1) = \left(\frac{i}{\hbar}\right)^3 \sum_{cba} V_{ad}V_{dc}V_{cb}V_{ba} \exp[-i(\varepsilon_d\tau_{43} + \varepsilon_c\tau_{32} + \varepsilon_b\tau_{21}) + f_{dcba}(\tau_4,\tau_3,\tau_2,\tau_1)] \quad (37)$$

where

$$f_{dcba}(\tau_4,\tau_3,\tau_2,\tau_1) = -g_{dd}(\tau_{43}) - g_{cc}(\tau_{32}) - g_{bb}(\tau_{21}) - g_{dc}(\tau_{42}) + g_{dc}(\tau_{43}) + g_{dc}(\tau_{32}) - g_{db}(\tau_{41}) + g_{db}(\tau_{42}) + g_{db}(\tau_{31}) - g_{db}(\tau_{32}) - g_{cb}(\tau_{31}) + g_{cb}(\tau_{32}) + g_{cb}(\tau_{21}). \quad (38)$$

Here

$$g_{\nu\nu'}(t) = \int_0^t d\tau_2 \int_0^{\tau_2} d\tau_1 C_{\nu\nu'}(\tau_2-\tau_1), \quad (39)$$

is the line broadening function, and

$$C_{\nu\nu'}(\tau_2-\tau_1) \equiv \langle Q_\nu(\tau_2)Q_{\nu'}(\tau_1)\rangle \quad (40)$$

is the cross correlation function of frequency fluctuations of levels ν and ν'. We note the symmetry $g_{\nu\nu'}(t) = g^*_{\nu'\nu}(-t)$. Upon the substitution of these results in Eqs. (13), (16), and (17) we can calculate $\chi^{(3)}$. Using the Brownian oscillator model for the correlations function we have [8]

$$g_{\nu\nu'}(t) = \left(\frac{2\lambda_{\nu\nu'}kT}{\Lambda^2_{\nu\nu'}} - i\frac{\lambda_{\nu\nu'}}{\Lambda_{\nu\nu'}}\right)[\exp(-\Lambda_{\nu\nu'}|t| - 1 + \Lambda_{\nu\nu'}|t|)]. \quad (41)$$

Here $\lambda_{\nu\nu'}$ represents the coupling strength (the variances of frequency fluctuations are $2\lambda_{\nu\nu'}kT$) and $\Lambda_{\nu\nu'}$ is the inverse time scale of bath fluctuations. For fast fluctuations $\Lambda^2 \gg 2\lambda kT$ we have

$$g_{\nu\nu'}(t) = \Gamma_{\nu\nu'}|t|, \quad (42)$$

with $\Gamma_{\nu\nu'} \equiv 2\lambda_{\nu\nu'}kT/\Lambda_{\nu\nu'}$. In the opposite limit of slow fluctuations $\Lambda^2 \ll 2\lambda kT$ we obtain

$$g_{\nu\nu'}(t) = \lambda_{\nu\nu'}kTt^2 - i\lambda_{\nu\nu'}|t|. \quad (43)$$

Equation (37) implies that Eq. (23) may not be generally factorized into three factors that depend on s_1, s_2, and s_3.

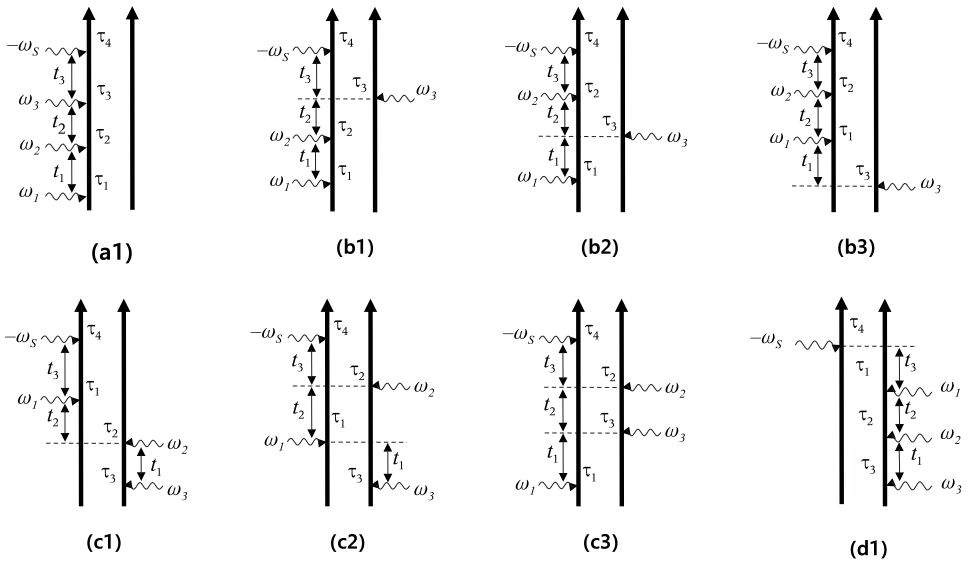

FIG. 3. The eight double-sided Feynman diagrams representing the Liouville space pathways contributing to $\chi^{(3)}$, Eq. (28). Complete time ordering of all interactions with the density matrix is maintained. t_1, t_2, and t_3 are the physical time intervals between successive interactions. Figs. 1(a) and 1(d) are time ordered and each gives only one time-ordered diagram (a_1 and d_1). Figs. 1(b) and 1(c) each split into three diagrams b_1, b_2, and b_3 and c_1, c_2, c_3. Altogether the four loop diagrams yield eight double-sided diagrams.

Similarly, Eq. (16) may not be factorized into factors that depend on t_1, t_2, and t_3; a threefold integration will be required to calculate $\chi^{(3)}$ in either representation.

As an example for a dramatic interference effect related to these factorizations, let us consider the level system with a ground state a and two closely lying excited states b and d. b and d can represent, for example, two vibrational states belonging to the same electronically excited state, or two Zeeman levels. The transition dipole only connects a with b and a with d. We look for two-photon resonances of the form $(\omega_1-\omega_2-\omega_{bd})$ in $\chi^{(3)}(-\omega_s;\omega_3,-\omega_2,\omega_1)$. These are a kind of Raman resonances, but for excited state frequencies ω_{bd}. For simplicity we tune ω_3 to be off resonant and assume the fast fluctuation limit equation (42). In this case the Green's functions assume the form

$$\mathcal{G}_{\nu\nu'}(\omega) = \frac{1}{\omega - \omega_{\nu\nu'} + i\Gamma_{\nu\nu'}}.$$

The two diagrams responsible for such resonances in the time-ordered expansion are shown in Fig. 4. They give the following contribution to $\chi^{(3)}$:

$$|V_{ab}|^2|V_{ad}|^2 \frac{1}{-\omega_s - \omega_{ba} + i\Gamma_{bb}} \frac{1}{\omega_1 - \omega_2 - \omega_{bd} + i\Gamma_{bd}} \times \left(\frac{1}{\omega_1 - \omega_{ba} + i\Gamma_{bb}} + \frac{1}{-\omega_2 - \omega_{ad} + i\Gamma_{dd}} \right). \quad (44)$$

Here

$$\Gamma_{bd} = (\Gamma_{bb} + \Gamma_{dd})(1-\eta), \quad (45)$$

$$\lambda_{bd} = \lambda_{dd}\lambda_{bb}(1-\eta), \quad (46)$$

and η is the correlation coefficient for fluctuations of ω_{ba} and ω_{da}. $\eta=-1,0,1$ represent fully anticorrelated, uncorrelated, and fully correlated fluctuations. The two terms in the brackets can be combined to give

$$\frac{\omega_1 - \omega_2 - \omega_{bd} + i(\Gamma_{bb} + \Gamma_{dd})(1 - \eta + \eta)}{(\omega_1 - \omega_{ba} + i\Gamma_{bb})(-\omega_2 - \omega_{ad} + i\Gamma_{dd})}. \quad (47)$$

Substituting this in Eq. (44) results in

$$|V_{ab}|^2|V_{ad}|^2 \frac{1}{-\omega_s - \omega_{ba} + i\Gamma_{bb}} \times \frac{1}{\omega_1 - \omega_{ba} + i\Gamma_{bb}} \frac{1}{-\omega_2 - \omega_{ad} + i\Gamma_{dd}} \times \left(1 + \eta \frac{1}{\omega_1 - \omega_2 - \omega_{bd} + i(\Gamma_{bb} + \Gamma_{dd})(1-\eta)} \right). \quad (48)$$

The desired resonance (second term in the bracket) contains an η prefactor and its width scales as $1-\eta$. When the fluctuations are uncorrelated ($\eta=0$), Eqs. (23) and (25) can be factorized and we expect no such resonances. Note that these resonances never show up in Eq. (32), but for $\eta=0$ cancel by

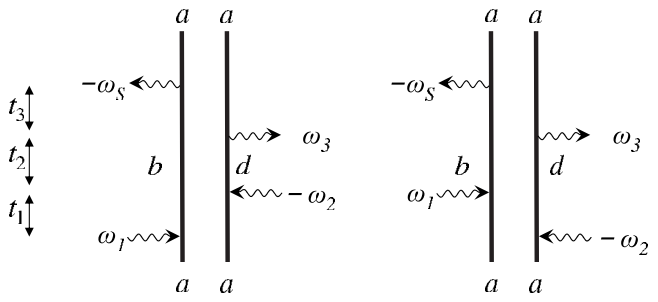

FIG. 4. The two double-sided diagrams which contribute to the correlation-induced resonance [Eq. (44)].

interference in Eq. (33). For finite η and fast fluctuations Eq. (33) can be factorized. Here, these resonances show up naturally in Eq. (33), but in Eq. (32) they come from the breakdown of the factorization. For $\eta=1$ the resonance width vanishes since there is no pure dephasing of the *bd* transition, Eq. (46). Such resonances have been observed both for collisional broadening in atomic vapors [15] and for phonon broadening in mixed molecular crystals [16] and were denoted "dephasing induced" [15–17]. The present calculation shows that more precisely they are induced by the correlations of fluctuations rather than the fluctuations themselves, and are associated with specific factorizations of the multipoint correlation functions.

VI. DISCUSSION

When nonlinear response functions are calculated using the density matrix, the n-order susceptibility has $2^n n!$ terms. These represent 2^n Liouville space pathways which keep track of the complete time ordering of the various interactions with the bra and the ket, combined with the $n!$ permutations of n frequencies representing all possible time-ordered interactions with the various fields. A wave-function loop calculation keeps track of time ordering only partially (relative time ordering of ket and bra interactions is not maintained). This gives $n+1$ terms, times the same $n!$ permutations for a total of $(n+1)!$ terms. This considerable reduction in the number of terms is very convenient for the frequency-domain response, where the bookkeeping of time ordering is not necessary anyhow.

When all field frequencies are tuned off resonance, we can neglect the imaginary part of the Green's function. We can then set $\mathcal{G}=\mathcal{G}^{\dagger}$ and use forward-only propagation. Equation (25) then assumes a more symmetric form

$$\chi^{(3)}(-\omega_s,\omega_1,\omega_2,\omega_3) = \sum_{p_4} \langle V_L \mathcal{G}(\Omega_3) V_L \mathcal{G}(\Omega_2) V_L \mathcal{G}(\Omega_1) V_L \rangle \times \delta(\Omega_1+\Omega_2+\Omega_3+\Omega_4), \tag{49}$$

p_4 denotes the summation over all 4! permutations of $\Omega_1,\Omega_2,\Omega_3,\Omega_4$ with $\omega_1,\omega_2,\omega_3,-\omega_s$. Figures 1(a)–1(d) correspond to the permutations $-\omega_s=\Omega_4,\Omega_3,\Omega_2$, and Ω_1, respectively. Now we have a single basic term with $(n+1)!$ permutations, as opposed to Eq. (25) where we have $(n+1)$ terms each containing $n!$ permutations [18].

The loop expansion is most adequate for many-body perturbation theory and involves a combination of forward and backward time evolution periods in Hilbert space. The density matrix calculation, in contrast, only requires a forward propagation, but it must be done in Liouville space. The time-domain response functions may be obtained by a threefold Fourier transform of $\chi^{(3)}$,

$$S^{(3)}(t_3,t_2,t_1) = \theta(t_3)\theta(t_2)\theta(t_1) \int\int\int d\omega_1 d\omega_2 d\omega_3 \times \chi^{(3)}(-\omega_s;\omega_1,\omega_2,\omega_3) \exp[-i\omega_1(t_1+t_2+t_3) - i\omega_2(t_2+t_3) - i\omega_3 t_3]. \tag{50}$$

By substituting Eq. (25) in Eq. (50) we can calculate the response function by transforming the compact frequency domain expression obtained by a diagrammatic expansion on the Keldysh loop.

ACKNOWLEDGMENTS

The support of the Chemical Sciences, Geosciences and Biosciences Division, Office of Basic Energy Sciences, Office of Science, U.S. Department of Energy is gratefully acknowledged. I wish to thank Christoph Marx for the careful reading of the manuscript and useful comments.

[1] H. Haug and A.-P. Jauho, *Quantum Kinetics in Transport and Optics of Semiconductors* (Springer-Verlag, Berlin, 1996).
[2] L. P. Kadanoff and G. Baym, *Quantum Statistical Mechanics. Green's Function Methods in Equilibrium and Nonequilibrium Problems* (Benjamin, Reading, MA, 1962).
[3] R. Mills, *Propagators for Many-Particle Systems; an elementary treatment* (Gordon and Breach, New York, 1969).
[4] J. Negele and H. Orland, *Quantum Many Particle Systems* (Westview Press, Boulder, CO, 1998).
[5] J. Rammer, *Quantum Field Theory of Non-Equilibrium States* (Cambridge, New York, 2007).
[6] L. V. Keldysh, Sov. Phys. JETP **20**, 1018 (1965).
[7] J. Schwinger, J. Math. Phys. **2**, 407 (1961).
[8] S. Mukamel, *Principles of Nonlinear Optical Spectroscopy* (Oxford University Press, New York, 1995).
[9] N. Bloembergen, *Nonlinear Optics* (Benjamin, New York, 1965).
[10] S. Mukamel, Phys. Rev. E **68**, 021111 (2003).
[11] U. Fano, Rev. Mod. Phys. **29**, 74 (1957).
[12] A. Ben-Reuven, Adv. Chem. Phys. **33**, 235 (1975).
[13] V. Chernyak, N. Wang, and S. Mukamel, Phys. Rep. **263**, 213 (1995).
[14] D. Abramavicius and S. Mukamel, Chem. Rev. (Washington, D.C.) **104**, 2073 (2004).
[15] A. R. Bogdan, M. W. Downer, and N. Bloembergen, Phys. Rev. A **24**, 623 (1981); L. J. Rothberg and N. Bloembergen, *ibid.* **30**, 820 (1984); L. Rothberg, in *Progress in Optics*, edited by E. Wolf (North-Holland, Amsterdam, 1987), Vol. 24, p. 38.
[16] J. R. Andrews and R. M. Hochstrasser, Chem. Phys. Lett. **82**, 381 (1981).
[17] R. Venkatramani and S. Mukamel, J. Phys. Chem. B **109**, 8132 (2005).
[18] J. F. Ward, Rev. Mod. Phys. **37**, 1 (1965); B. J. Orr and J. F. Ward, Mol. Phys. **20**, 513 (1971).